Journal of Alloys and Compounds 509 (2011) 1401–1406

Contents lists available at ScienceDirect

Journal of Alloys and Compounds

journal homepage: www.elsevier.com/locate/jallcom

YPd_2Al_3—A new superconducting compound

Jiří Pospíšil*, Marie Kratochvílová, Martin Diviš, Jan Prokleška, Jana Poltierová Vejpravová, Vladimír Sechovský

Charles University Prague, Faculty of Mathematics and Physics, Department of Condensed Matter Physics, Ke Karlovu 5, 121 16 Prague, Czech Republic

ARTICLE INFO

Article history:
Received 26 July 2010
Received in revised form 29 October 2010
Accepted 29 October 2010
Available online 10 November 2010

Keywords:
REPd_2Al_3
YPd_2Al_3
Superconductivity
Electronic structure calculations

ABSTRACT

We have prepared a polycrystalline sample of YPd_2Al_3 – a so far unknown member of the well-known group of intermetallic compounds *RE*Pd_2Al_3 (*RE* = rare earth elements). The XRPD analysis revealed that the YPd_2Al_3 compound crystallizes in the hexagonal crystal structure adopted by the entire *RE*Pd_2Al_3 family, too. For the new material we have measured the magnetization, AC susceptibility, specific heat and electrical resistivity with respect to temperature and magnetic field. We have observed superconductivity with $T_{SC} \approx 2.2$ K in well-annealed samples and Pauli paramagnetism in normal state. We have also performed *ab initio* electronic structure calculations and found reasonable agreement between experimental findings and corresponding results of theoretical calculations.

1. Introduction

An important stimulation of interest in physics of the *RE*Pd_2Al_3 compounds provided the discovery of the isostructural heavy-fermion superconductors UPd_2Al_3 ($\gamma = 150$ mJ K^{-2} mol^{-1}, $T_{SC} = 2$ K, $T_N = 14$ K, and UNi_2Al_3 [1–3]) where superconductivity coexists with quite large antiferromagnetically ordered U moments of 0.85 μ_B (UPd_2Al_3) [1]. All these 123 intermetallics adopt the same hexagonal $PrNi_2Al_3$-type crystal structure [4,5]. The *RE*Pd_2Al_3 family exhibits a broad range of types of magnetic ordering, which are strongly influenced by crystal field (CF) interactions [6,7]. The non-f-electron compound $LaPd_2Al_3$ displays a superconducting transition (SC) at temperature 0.8 K [8]. $CePd_2Al_3$ exhibits heavy-fermion behavior ($\gamma = 380$ mJ K^{-2} mol^{-1}) with a strong Kondo effect [9–11]. $PrPd_2Al_3$ remain paramagnetic down to 1.5 K [12]. $NdPd_2Al_3$ undergoes an antiferromagnetic transition around 6.5 K [11].

The experimental data observed for $SmPd_2Al_3$ point to a complex phase diagram in the temperature range below 12 K, characterized by multiple magnetic phase transitions. The $SmPd_2Al_3$ magnetism is strongly influenced by the crystal field interactions. The paramagnetic susceptibility behavior reflects population of the higher energy multiplets of the Sm^{3+} ion [13].

Magnetism of $GdPd_2Al_3$ is rather complex, as well. Experimental data document magnetic phase transitions at 13 and 16 K, respectively. The low-temperature magnetic ordering has been conceived in terms of a two-dimensional triangular lattice antiferromagnet [14,15].

In the course of investigations of magnetism in the *RE*Pd_2Al_3 (*RE* = rare earth elements – La, Ce, Pr, Nd, Sm, Gd) intermetallic compounds we felt a need of another non-f-electron analogue besides $LaPd_2Al_3$, namely YPd_2Al_3. Since the latter compound has not been yet reported we faced the problem of performing entire metallurgy and structure study of such material followed by investigation of magnetic, transport and thermodynamic properties with respect to temperature and applied magnetic fields. For closer understanding of physics of YPd_2Al_3 we have also performed *ab initio* electronic structure calculations for this material.

2. Experimental and computational details

The polycrystalline sample of YPd_2Al_3 has been prepared by melting the stoichiometric amounts of elements (purity of Y – 99.9%, Pd – 99.95%, Al – 99.9999%) in an arc-furnace under the high-purity (6N) argon atmosphere. The sample was re-melted several times to ensure good homogeneity. No significant evaporation was observed during melting. Half of the sample was subsequently wrapped in a tantalum foil, sealed in silica tubes under the vacuum 10^{-7} mbar, and annealed at 700 °C for 14 days and then slowly cooled to avoid internal stresses. Both the samples (as cast and annealed) were characterized by the X-ray powder diffraction (XRPD) method. The XRPD patterns have been recorded at room temperature on a Seifert diffractometer equipped with a monochromator providing the Cu Kα radiation. The diffraction patterns were evaluated by the standard Rietveld technique using the FullProf/WinPlotr software [16,17]. The sample composition has been verified by FE-EDX analysis. The samples of shapes appropriate for all measurements were prepared using a wire saw to prevent additional stresses in the samples.

The sample for resistivity measurement was prepared in the shape of a small block ($1 \times 0.5 \times 4$ mm^3). The sample for heat capacity measurement was prepared in the shape of a small plate $1.5 \times 1.5 \times 0.5$ mm^3. The electrical resistivity was measured as a function of temperature and magnetic field by using four terminal AC method. Relaxation method was used for heat capacity measurements. The AC

* Corresponding author. Tel.: +420 22191 1352; fax: +420 22491 1061.
E-mail address: jiri.pospisil@centrum.cz (J. Pospíšil).

0925-8388/$ – see front matter © 2010 Elsevier B.V. All rights reserved.
doi:10.1016/j.jallcom.2010.10.193

Table 1
Lattice parameters of whole series $REPd_2Al_3$ compound.

Compound	a (Å)	c (Å)	Ref.
YPd_2Al_3 as-cast	5.372 ± 0.001	4.193 ± 0.002	[Actual work]
YPd_2Al_3 annealed	5.3704 ± 0.0006	4.1932 ± 0.0007	[Actual work]
$LaPd_2Al_3$	5.5082	4.2267	[4]
$CePd_2Al_3$	5.4709	4.2157	[5]
$PrPd_2Al_3$	5.4569	4.2117	
$NdPd_2Al_3$	5.4419	4.2069	
$SmPd_2Al_3$	5.4131	4.1997	
$GdPd_2Al_3$	5.3924	4.1941	
UPd_2Al_3	5.3650	4.1860	

susceptibility and electrical resistivity were measured also with a ^{3}He option at temperatures down to 350 mK. AC susceptibility was measured using home-made magnetometer, where we used a piece of tin shaped similar to our sample as a standard for demonstration of the bulk superconducting state. The measurement works based on the response of the sample to the AC magnetic field. Details of the equipment are published in [18]. All measurements were performed using a PPMS (Physical Property Measurement System, produced by Quantum Design) and MPMS (Magnetic Property Measurement System, produced by Quantum Design) devices.

To obtain reliable information about the ground state electronic structure and related properties we have applied first principles theoretical methods. The ground state electronic structure was calculated on the basis of density functional theory (DFT) within local spin density approximation (LSDA) [19] and the generalized gradient approximation (GGA) [20,21]. For this purpose, we used the full potential augmented plane wave plus local orbitals method (APW+lo) as implemented in the latest version (WIEN2k) of the original WIEN code [22]. The calculations were scalar relativistic. The calculations were performed with the following parameters. Nonoverlapping atomic sphere (AS) radii of 2.8, 2.5 and 2.0 a.u. (1 a.u. = 52.9177 pm) were taken for Y, Pd and Al, respectively. The basis for expansion of the valence states (<6 Ry below the Fermi energy) consisted of more than 800 basis functions (more than 130 APW/atom) plus Y (4s, 4p), Pd (4s, 4p) and Al (2p) local orbitals. The Brillouin zone (BZ) integrations were performed with the tetrahedron method [22], on a 243 special k-point mesh (4000 k-points in the whole BZ). We carefully tested the convergence of the results presented with respect to the parameters mentioned and found them to be sufficient for all presented characteristics of YPd_2Al_3 compound.

3. Results and discussion

We have successfully synthesized a polycrystalline sample of the YPd_2Al_3 compound. Small pieces of the as-cast and annealed sample, respectively, were powdered in agate mortar and XRPD data were collected. We did not observe any significant difference between patterns of as-cast and annealed sample. Practically all reflections can be assigned to the $PrNi_2Al_3$-type structure type, i.e. YPd_2Al_3 crystallizes in the hexagonal crystal structure belongs to the space group $P6/mmm$. The determined lattice parameters for this compound at room temperature $a = 5.372 \pm 0.001$ Å, $c = 4.193 \pm 0.002$ Å (as-cast sample) $a = 5.3704 \pm 0.0006$ Å, $c = 4.1932 \pm 0.0007$ Å (annealed sample) are close to values for $GdNi_2Al_3$ and UNi_2Al_3 as can be seen in Table 1.

There were few additional reflections observed in the powder pattern besides these corresponding to the YPd_2Al_3 structure signalizing presence of a spurious phase in the sample. The intensity of reflections appertain to impurities was slightly suppressed in the annealed sample pattern in comparison to as-cast one. The change of lattice parameters and volume cell after annealing was negligible (see Table 1). Subsequently, we have performed FE-EDX analysis on different locations of the annealed sample. The elementary analysis confirmed the majority of YPd_2Al_3 compound in all surveyed samples. Two types of spurious phases have been identified. We have analyzed, in particular tiny amounts of Y_2O_3 and probably a non-stoichiometric compound with the composition close to YPd_6Al_3. The impurities were localized mainly on grain boundaries (see Fig. 1). These compounds can be responsible for the additional reflections in XRPD patterns. We have carried out the area analysis and concentrations gradients have been studied as well. We have not recorded any concentrations gradients and hence we expect uniform distribution of all elements. The results

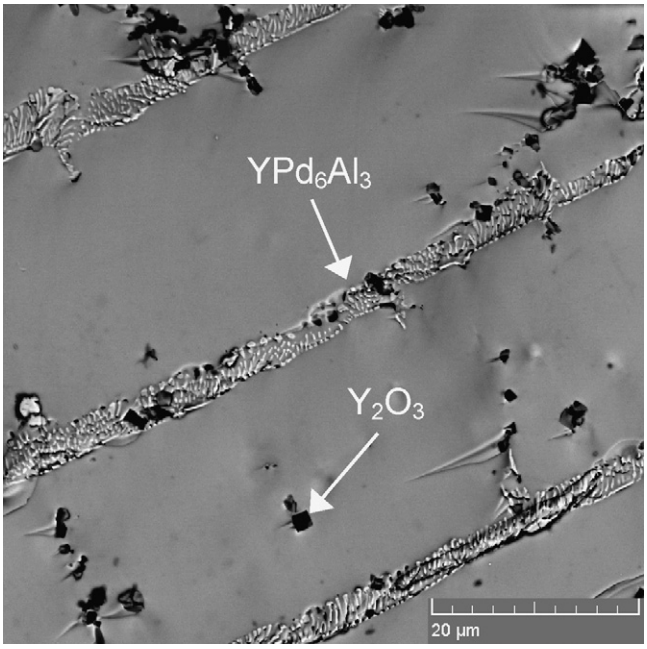

Fig. 1. Picture of surface of the annealed sample from Scanning Electron Microscope with use BSE detector to emphasis the phase composition. The small white grains are the nonstoichiometric phase of YPd_6Al_3. The square black grains are Y_2O_3.

of EDX analysis support the results of XRPD and declare majority of amount of the YPd_2Al_3 compound. Generally, the structure analysis confirmed, that the annealing process at 700 °C led to only minor crystallographic material changes, although it was enough to change significantly physical properties as will be presented further.

We measured resistivity data of the as-cast and annealed samples and we have observed significantly different behavior (see Fig. 2). The temperature of the superconducting transition of the as-cast sample was observed to be only 0.6 K while a considerably higher temperature of the superconducting transition $T_{SC} = 2.2$ K was found for the annealed sample. The temperatures of SC transitions were established as a maximum of the curve of temperature dependence of dR/dT. The main reason of so significantly different behavior between as-cast and annealed sample can be material stress and imperfect occupancy of atoms after sample melting.

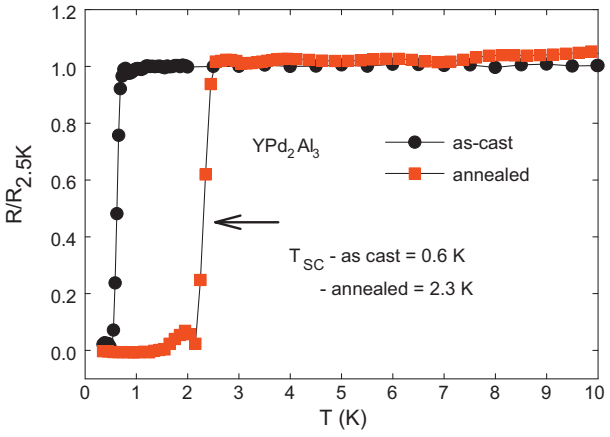

Fig. 2. Temperature evolution of the electrical resistivity of the as-cast and annealed sample, respectively, with apparent drop of the resistivity to 0 at T_{SC}. The temperature of SC transition of the annealed sample $T_{SC} = 2.3$ K is significantly higher than for as-cast sample $T_{SC} = 0.6$ K.

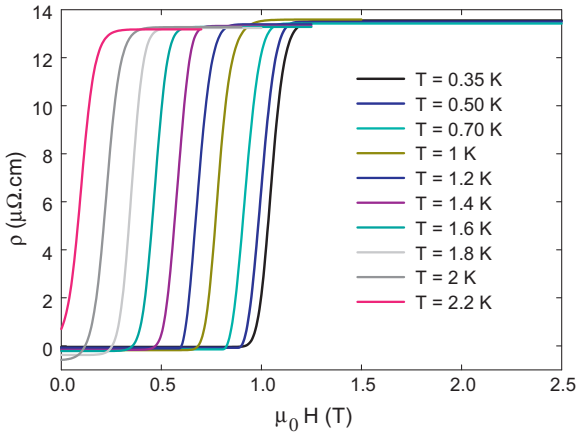

Fig. 3. Magnetoresistance curves measured at various temperatures.

The magnetoresistance data reflect the typical suppression of the superconducting state by the magnetic field accompanied by decreasing T_{SC} with increasing field as is shown in the Fig. 3. We have determined the values of the critical fields at various temperatures from available magnetoresistance data. The values of critical fields were taken as the maximum of the magnetic field dependence of $dR/d\mu_0 H$. The critical fields are plotted in Fig. 4 (square dots). From the square law (Eq. (1))

$$\mu_0 H_{C2}(T) = \mu_0 H_{C2}(0)\left[1 - \left(\frac{T}{T_{SC}}\right)^2\right] \quad (1)$$

we have calculated the value $\mu_0 H_{C2}(0)$ = 1.25 T. We found, that the square law is not a suitable fit for the critical fields obtained from the magnetoresistance. We have also tried to estimate the value $\mu_0 H_{C2}(0)$ from Werthamer–Helfand–Hohenberg (WHH) formula (Eq. (2)) [23] within the weak-coupling BCS theory, as well.

$$\mu_0 H_{C2}(0) = -0.693\left(\frac{dH_{C2}}{dT_{T=T_{SC}}}\right) T_{SC} \quad (2)$$

We have found value $\mu_0 H_{C2}(0)$ = 960 mT based on WHH, which is value closer to value found later using square law. We have estimated the superconducting coherence length $\xi(0)$ based on Ginzberg–Landau formula for an isotropic tree-dimensional superconductor (Eq. (3)).

$$\mu_0 H_{C2}(0) = \frac{\Phi_0}{2\pi\xi(0)^2} \quad (3)$$

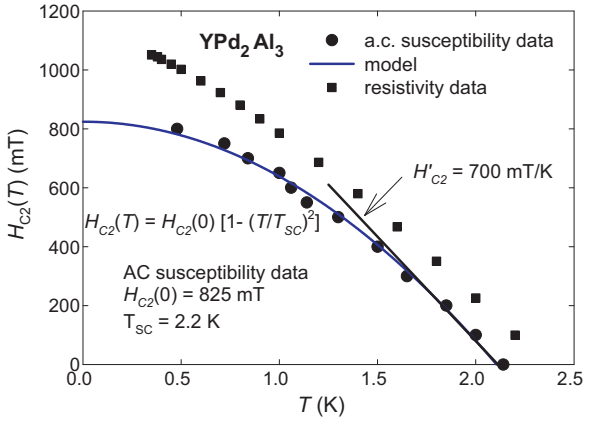

Fig. 4. Evolution of the critical magnetic field measured obtained from resistivity and AC susceptibility measurements.

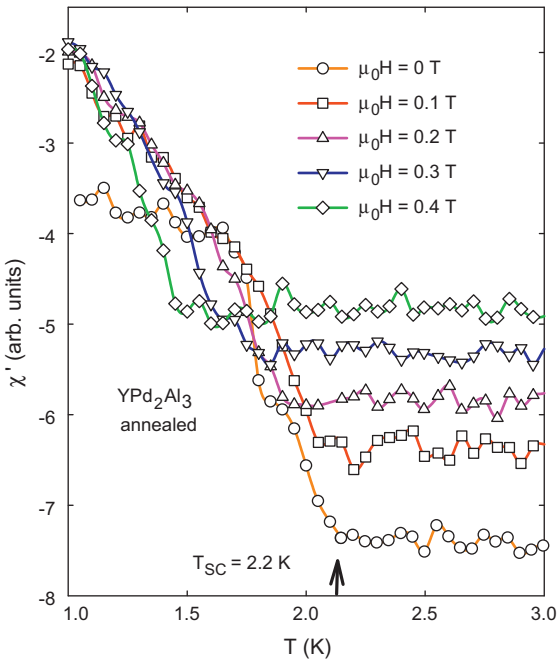

Fig. 5. The picture shows the temperature evolution of the AC susceptibility in various magnetic fields. Sharp steps on curves are visible at temperatures, when the YPd_2Al_3 sample become superconducting and consequently are macroscopically diamagnetic. To clarify the figure, only selected curves are plotted.

We found the coherence length $\xi(0)$ = 192 Å.

The deviation of the $\mu_0 H_{C2}$(T) out from resistivity from square law carry motivated us to measure existence superconductivity using AC susceptibility.

The home-made AC magnetometer was used to found out the temperature, where the annealed sample is macroscopically in the superconducting state. The measurement was performed for the same annealed sample, which was used for resistivity measurements. The result of this experiment is shown in the Fig. 5. We have used comparable piece of tin as a standard during measurement. We found sharp step at 3.7 K, which corresponded with superconducting transition of the tin (data not shown). Whereas the transition of the tin was sharp, we have found broaden transition in the temperature range 2.2–1.7 K for YPd_2Al_3 compound. It can be induced by mechanical stress inside the sample and small composition inhomogeneities. Unfortunately we cannot perform fine measurement to obtain value of the Meissner fraction properly (for example like Ref. [24]). We are only able to compare the relative value change of the AC susceptibility between the standard (tin) and the sample in case of our home-made magnetometer. The susceptibility change was similar to SC transition of the similar piece of the tin although the transition of the YPd_2Al_3 compound was broadened. We suppose that majority part of the sample was in the SC state. The temperature of the superconducting transition of YPd_2Al_3 is marked by arrow at temperature 2.2 K. We verified this temperature by the AC susceptibility measurement using SQUID magnetometer, as well. The result is displayed in Fig. 6. The onset of the real part of AC susceptibility at 2.1 K corresponds to the result from the home-made AC magnetometer. The maximum of the imaginary part is slightly below 2 K.

All the values of the critical field from different experiments are plotted together in Fig. 4. The circles represent results of AC susceptibility measurements. The colored curve represents the square-law fit. The significant deviation of the resistivity data from the square law is clearly visible as was discussed earlier, whereas the AC measurement provided much better result, where the square law is a very good approximation. The temperature of

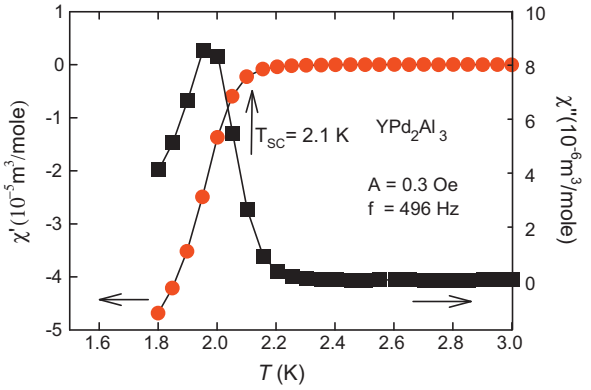

Fig. 6. Temperature dependence of real and imaginary part od AC susceptibility. The black arrow marks T_{SC} – 2.1 K in the curve of real part of AC susceptibility.

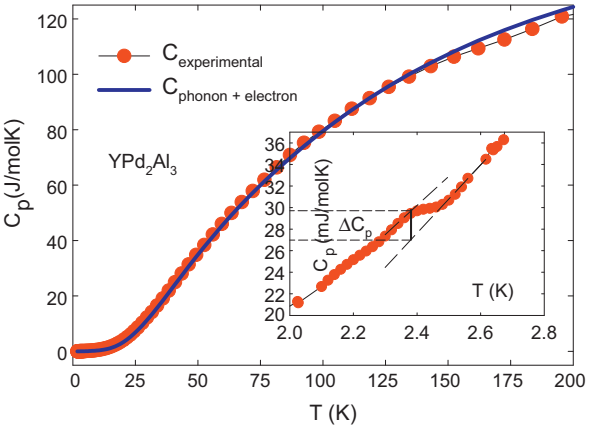

Fig. 7. Temperature dependence of the specific heat of the annealed sample. The blue curve represents model based on Debye and Einstein model. The low temperature detail is shown in the inset of the figure.

the superconducting transition in zero field is T_{SC} = 2.2 K according to AC susceptibility data. We have also determined the value of the critical field $H_{C2}(0)$ = 825 mT from AC data, which is lower than the corresponding result from resistivity data.

Specific heat data measured on annealed sample confirmed superconductivity transition as well as AC and resistivity data although the peak at temperature of SC transition was really weak (see inset of Fig. 7) We have fitted the temperature dependence of the specific heat based on Einstein and Debye model using Eq. (4) with correction to anharmonicity. The values of Debye and Einstein temperatures and degeneracy of Einstein modes are listed in Table 2. The phonon spectrum is similar to lanthanide analogs (see Ref. [12]). We fitted the C_p/T vs. T^2 data by a linear function and we obtained the value of Sommerfeld coefficient γ = 7.2 mJ/mol K^2 (Eq. (5)), which denoted a quite low density of states at Fermi level.

$$C_{ph} = R\left(\frac{1}{1-\alpha_D T}C_D + \sum_{i=1}^{3N-3}\frac{1}{1-\alpha_{Ei}T}C_{Ei}\right) \quad (4)$$

Table 2
Phonon spectrum of YPd_2Al_3 compound obtained based on Debye and Einstein model.

Branches	Degeneracy	Θ (K)	α (10^{-4} K^{-1})
θ_D		200	1.0
θ_{E1}	3	380	2.0
θ_{E2}	5	211	1.0
θ_{E3}	2	130	2.0
θ_{E4}	5	550	2.0

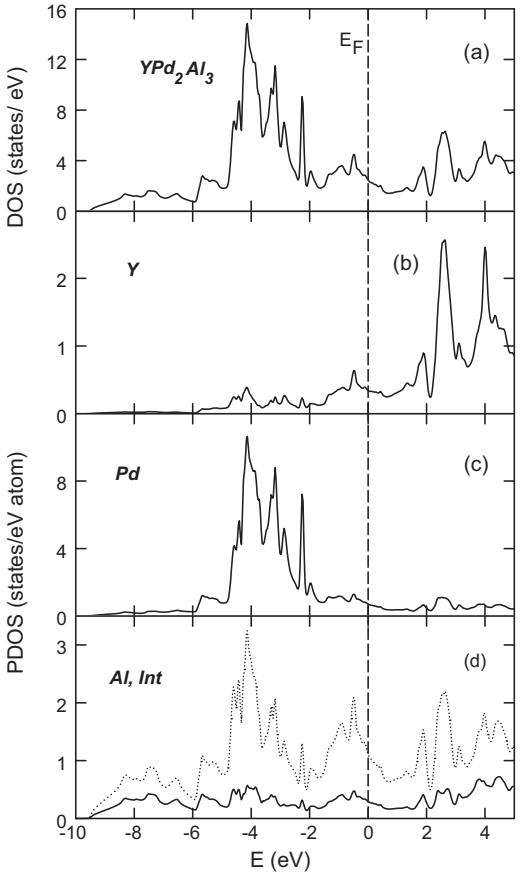

Fig. 8. Total DOS (a) and atom-projected DOS [(b)–(d)] of YPd_2Al_3. The projected Y DOS [(b) bold line], Pd [(c) bold line], Al [(d) bold line], and the interstitial region [(d) dashed line] are shown. Fermi level is adjusted at zero energy.

$$C_e = \frac{2nk_B^2 T}{E_F} = \gamma T \quad (5)$$

We have tried to estimate the value of the $(\Delta C_p)_{T_{SC}}/\gamma T_{SC}$, which should be 1.43 based on *BSC* weak-coupling theory. We have found value 0.2, which is lower than is expected. We suppose that the sample did not reach the SC state at one certain temperature and the SC transition is broadened due to the existence of the mechanical stress inside the sample. It can be reason of the so anomaly weak jump in the specific heat data, which is broaden to certain temperature region because the AC susceptibility data shown broaden transition, as was discussed earlier.

The experimental magnetic susceptibility in the normal state is temperature independent and the value is close to 1.9×10^{-8} m^3/mol. The theoretical value of 7.7×10^{-8} m^3/mol calculated by using well-known equation for Pauli susceptibility (Eq. (6)) provides only right order with the experimental value. The overestimation of theoretical value is probably connected with approximate exchange correlation functional used in our first principles DFT calculations.

$$\chi = \mu_B^2 N(E_F) \quad (6)$$

The total density of electronic states (DOS) from GGA calculations at experimental equilibrium is shown for YPd_2Al_3 in Fig. 1a. The occupied part of the DOS has a width of 9.5 eV. The lowest band region, from −9.5 to −4.8 eV, originates mainly from free electron like states from the interstitial region and the Y 5s, Pd 5s, Al 3s and Al 3p states from the AS spheres (see Fig. 8b–d). The following band group from −4.8 eV to the Fermi level represents mainly the Pd 4d states hybridizing with the Y 4d and Al 3p states. The

unoccupied states above the Fermi level have predominantly the Y 4d character with an admixture of the Pd 4d and Al 3p states and the large contribution from the free-electron like interstitial region (Fig. 8b–d). We performed also the spin polarized LSDA and GGA calculations in order to estimate the value of the hybridization induced Pd and Al magnetic moments and found negligible values. The Fermi level for YPd_2Al_3 situated at the descending part of the DOS yielded $N(E_F) = 2.56$ states/eV. The orbital analysis of the DOS shows that mainly the Pd 4d, Y 4d and Al 3p states contribute to the total DOS at E_F. The value of the DOS at E_F is too small to cause a spontaneous magnetic polarization of the Pd 4d states. The value of the DOS at E_F for YPd_2Al_3 corresponds to an electronic specific heat coefficient $\gamma = 6.0\,\mathrm{mJ\,mol^{-1}\,K^{-2}}$, which is somewhat lower than the γ value of $7.2\,\mathrm{mJ\,mol^{-1}\,K^{-2}}$ derived from our specific heat data. This points to a rather low value of the mass-enhancement coefficient $\lambda = 0.19$ for YPd_2Al_3 ($\gamma_{exp} = (1+\lambda)\,\gamma_{band}$) indicating a weak electron–phonon interaction in the YPd_2Al_3 compound.

The first superconducting temperature (T_{SC}) relation presented by McMillan [25] is based on the minimum set of three parameters (averaged Debye temperature θ_D, mass-enhancement coefficient λ and a Coulomb pseudopotential μ^*), which found extensive applications in the analysis of superconductors. Starting with the full Eliashberg equations, McMillan introduced ad hoc assumptions on the nature of the spectral function and assumed further that T_{SC} depends on spectral function only through λ. Performing numerical solutions of the Eliashberg equations McMillan derived so-called "McMillan-formula" (Eq. (7)) [25].

$$T_C = \frac{\Theta_D}{1.45}\exp\left(-\frac{1.04\,(1+\lambda)}{\lambda - \mu^*\,(1+0.62\lambda)}\right) \tag{7}$$

Using Debye temperature $\theta_D = 200$ K obtained from specific heat data, mass-enhancement coefficient $\lambda = 0.19$ and a Coulomb pseudopotential $\mu^* = 0.13$ we have found T_{SC} less than 1 mK. We note that result from McMillan formula is especially very sensitive to the particular value of the mass-enhancement coefficient λ which is the result of our combined analysis of experimental specific heat data end first-principles calculations based on the DFT with approximate exchange correlation functional. For example the value of $\lambda = 0.6$ gives $T_{SC} \sim 1$ K which is quite close to our experimental value $T_{SC} = 2.1$ K. We also point out that we used Coulomb pseudopotential $\mu^* = 0.13$ which is a common practice to follow suggestion of McMillan for all transition metals and their compounds [25]. Therefore our calculations using McMillan formula can be taken as a starting crude estimate of T_{SC} only. One possible reason of limited applicability of McMillan formula for YPd_2Al_3 might be a complex nature of the phonon spectra in YPd_2Al_3. The actual high value of T_{SC} can be tentatively attributed to the coupling of electrons to special phonon modes. Therefore full first-principles calculations of the superconducting temperature T_{SC} of YPd_2Al_3 is desired although but this task is clearly beyond the scope of the present paper.

We now like to compare the performance of LSDA and GGA with respect to the equilibrium volume of YPd_2Al_3. The theoretical c/a ratio was calculated and found to almost coincide with the experimental one. Therefore the experimental c/a ratio was used and kept constant in the calculations. The LSDA value of equilibrium volume is smaller and deviates from the experimental value by more than four percent. This is a typical deviation usually obtained in LSDA calculations. Both the GGA methods [20,21] tested in this work perform better than LSDA. The GGA from Ref. [20] is superior and provides the volume $V/V_0 = 0.99$ larger than LSDA gives. Finally the GGA from Ref. [21] is overestimating the experimental volume and provides the $V/V_0 = 1.017$.

Table 3
Superconducting and other parameters for YPd_2Al_3.

Parameter	Value
T_{SC} specific heat	2.45 K
T_{SC} resistivity	2.3 K
T_{SC} AC susceptibility	2.2 K
T_{SC} theoretical	<0.001 K
$\mu_0 H_{C2}(0)$ WHH	960 mT
$\mu_0 H_{C2}(0)$ square law	825 mT
γ experimental	$7.2\,\mathrm{mJ\,mol^{-1}\,K^{-2}}$
γ theoretical	$6.0\,\mathrm{mJ\,mol^{-1}\,K^{-2}}$
$\xi(0)GL$	192 Å
$\Delta C/\gamma T_{SC}$	0.2
θ_D	200 K
λ	0.19

4. Conclusions

We have successfully synthesized the YPd_2Al_3 compound in polycrystalline form and found this material to be superconducting at temperature 2.2 K. The unit cell size is close to that of $GdPd_2Al_3$ to heavy lanthanides and is in very good agreement with our theoretical DFT value obtained using GGA [20]. The low value of the coefficient $\gamma = 7.2\,\mathrm{mJ/mol\,K^2}$ denotes the low density of state at Fermi level, which was confirmed by theoretical calculations, showing when the 4d-states of Y ion are 2–4 eV above the Fermi level. We also revealed a low mass enhancement ($\lambda = 0.19$), which indicates a weak electron-phonon interaction. According the straightforward use of McMillan formula the theoretical value of the superconducting temperature is too low below 1 mK. Therefore we tentatively propose that the observed superconductivity might for example result from the coupling of electrons to special phonon modes in the YPd_2Al_3 complex phonon spectra. All superconducting and other parameters for YPd_2Al_3 compound are digestedly presented in the Table 3.

Acknowledgments

This work is a part of the research plan MSM 0021620834 that is financed by the Ministry of Education of the Czech Republic. This work was also supported by the Czech National Foundation, grant nos: 202/09/1027, 202/09/H041 and 202/09/P354.

References

[1] C. Geibel, C. Schank, S. Thies, H. Kitazawa, C.D. Bredl, A. Böhm, M. Rau, A. Grauel, R. Caspary, R. Helfrich, U. Ahlheim, G. Weber, F. Steglich, Z. Phys. B 84 (1991) 1–2.
[2] C. Geibel, A. Bohm, R. Caspary, K. Gloos, A. Grauel, P. Hellmann, R. Modler, C. Schank, G. Weber, F. Steglich, Physica B 186–188 (1993) 188–194.
[3] C. Geibel, U. Ahlheim, C.D. Bredl, J. Diehl, A. Grauel, R. Helfrich, H. Kitazawa, R. Kohler, R. Modler, M. Lang, C. Schank, S. Thies, F. Steglich, N. Sato, T. Komatsubara, Physica C 185–189 (1991) 2651–2652.
[4] A. Dönni, A. Furrer, E. Bauer, H. Kitazawa, M. Zolliker, Z. Phys. B 104 (1997) 403–409.
[5] A. Dönni, A. Furrer, H. Kitazawa, M. Zolliker, J. Phys.: Condens. Matter 9 (1997) 5921–5933.
[6] S. Mentink, N. Bos, G. Nieuwenhuys, A. Menovsky, J. Mydosh, Physica B 186–188 (1993) 497.
[7] H. Ghosh, S. Ramakrishhnan, A. Chinchure, V. Marathe, G. Chandra, Physica B 223–224 (1996) 354.
[8] V.S. Zapf, R.P. Dickey, E.J. Freeman, C. Sirvent, M.B. Maple, Phys. Rev. B 65 (2001) 024437.
[9] S. Suga, M. Takeda, Y. Mori, N. Shino, S. Imada, H. Kitazawa, Physica B 186–188 (1993) 63–65.
[10] K. Ghosh, S. Ramakrishnan, S.K. Malik, G. Chandra, Phys. Rev. B 48 (1993) 6249.
[11] A. Dönni, H. Kitazawa, P. Fischer, T. Vogt, A. Matsushita, Y. Iimura, M. Zolliker, J. Solid State Chem. 127 (1996) 169–177.
[12] G. Motoyama, T. Nishioka, N. Sato, J. Phys. Soc. Jpn. 71 (2002) 1609.
[13] J. Pospíšil, M. Kratochvílová, J. Prokleška, M. Diviš, V. Sechovský, Phys. Rev. B 81 (2010) 024413.
[14] H. Kitazawa, K. Hashi, H. Abe, N. Tsujii, G. Kido, Physica B 294–295 (2001) 221–224.

[15] T. Inami, N. Terada, H. Kitazawa, O. Sakai, J. Phys. Soc. Jpn. 78 (2009) 084713.
[16] H. Rietveld, J. Appl. Crystallogr. 2 (1969) 65.
[17] http://www.ill.eu/sites/fullprof/.
[18] J. Prokleška, J. Pospíšil, J. Vejpravová Poltierová, V. Sechovský, J. Šebek, J. Phys.: Conf. Ser. 200 (2010) 012161.
[19] J.P. Perdew, Y. Wang, Phys. Rev. B 45 (1992) 13244.
[20] Z. Wu, R.E. Cohen, Phys. Rev. B 73 (2006) 235116.
[21] J.P. Perdew, K. Burke, M. Ernzerhof, Phys. Rev. Lett. 77 (1996) 3865.
[22] P. Blaha, K. Schwarz, G. Madsen, D. Kvasnicka, J. Luitz, in: K. Schwarz (Ed.), WIEN2k, an Augmented Plane Wave + Local Orbitals Program for Calculations Crystal Properties, TU Wien, Austria, 2001, ISBN 3-9501031-1-2.
[23] N.R. Werthamer, E. Helfand, P.C. Hohenberg, Phys. Rev. 147 (1966) 295.
[24] T. Nagano, Y. Tomioka, Y. Nakayama, K. Kishio, K. Kitazawa, Phys. Rev. B 48 (1993) 9689.
[25] W.L. McMillan, Phys. Rev. 167 (1968) 331.